Journal of the Korean Nuclear Society
Volume 15, Number 1 March, 1983

《**Original**》

Buoyancy Effects on Turbulent Mixing in the LMFBR Outlet Plenum

Soon Heung Chang

Korea Advanced Institute of Science and Technology

(Received January 25, 1983)

LMFBR 출구 공간에 있어서의 난류 혼합에 미치는 부력 효과

장 순 흥

한국과학기술원

(1983. 1. 25 접수)

Abstract

The effect of flow stratification is of particular concern during transient after scram in the outlet plenum of LMFBR. In this case, buoyancy effects on turbulent mixing are of importance to designers. An investigation has been made to identify the appropriate change in the available turbulence models which are necessary to include the effects of buoyancy on turbulence transport equations. The developed physical model of the buoyant turbulent flow are solved through SMAC method. Testing of the developed numerical model was undertaken and compared with experimental results. The results show that the buoyant turbulent effects account for a significant increase in the stability of the stratification, with a strong suppression of turbulence in the outlet plenum.

요 약

Scram이 일어난 후 과도 기간 동안 LMFBR 출구공간에 있어서의 유동성층의 영향은 특별한 문제로 제기되고 있다.

이러한 경우에 난류 혼합에 미치는 부력 효과는 설계자에게 중요하다. 난류 유동 방정식에 부력 효과를 갖지 않는 기존 난류 모형의 부력효과를 더하기 위한 연구가 행해졌다.

개발된 부력 난류 유동의 물리적 모형은 SMAC 수치 해석 방법을 통하여 풀어졌다.

개발된 수치 해석 모형이 시험되어졌고, 실험자료와도 비교되었다. 결과는 난류에 대한 부력 효과가 출구공간에서 난류를 강하게 억압하며 성층의 안정도를 상당히 증가시켰다.

Nomenclature

u,v	mean velocities
P	pressure
ρ	density
ρ_0	reference density

g_r, g_z	components of gravitational acceleration
R_r, R_z	the model resistance terms
SI	one fourth the square of the rate of strain tensor
k	turbulence kinetic energy
σ	turbulence kinematic viscosity
I	specific internal energy
γ_r	reciprocal of the Prandtl number
α, τ, τ_1	turbulence parameters
$\overline{U_i' T'}$	correlation of fluctuating velocity and temperature

I. Introduction

The effect of flow stratification is of particular concern during the transient-after-scram in the outlet plenum of the LMFBR. After a scram, the core effluent temperature decreases abruptly. If the cooler sodium has insufficient inertia to overcome the negative buoyancy force when entering the plenum, stratification followed by thermal shock can ensue.

To deal with and mitigate these thermal shock effects, an accurate prediction of the fluid velocities and temperature in the outlet plenum fields during the transient is necessary. For this purpose, the proper physical and numerical modellings of the recirculating buoyant turbulent flow are required.

Turbulent flows are three-dimensional and time dependent and are governed by the Navier-Stokes equations. But no practical numerical treatment can span all the time and length scales of turbulence. Therefore, we use ensemble-averaged equations with nonlinear terms $\overline{u_i' u_j'}$ and $\overline{u_i' T'}$ appearing in the resulting equations. A turbulence model is needed to relate these nonlinear terms to the time-averaged primitive variables: this is the fundamental problem of turbulence closure.

Recirculating turbulent flows are characterized by two following properties[1]. First, there is no single predominant direction of motion; indeed backflow is usually present in the chosen coordinates. Second, turbulent diffusive transport is important in both coordinate directions. Correspondingly, recirculating flows are thus governed by elliptic differential equations. In flows governed by elliptic differential equations, there is an even stronger reason for determining the length scale (l) from a transport equation. In recirculating flows, convective transport of l may be large. So, convective transport is important; and it is much more difficult than in boundary-layer flows to determine the length-scale profile by measurement.

To calculate a two-dimensional recirculating flow, the dependent variables and associated coefficients must be stored in two-dimensional arrays. Storage limitations may be present; also, the cost of making the calculations will usually be significant. There is thus strong incentive to keep the number of turbulence transport equationsas as small as possible and to avoid making a detailed calculation of the low-Reynolds number region close to the wall. For this reason, two-equation turbulence model is adopted in this work.

Two-equation models determine k, the turbulence kinetic energy and l, the length scale, from transport equations. Then, $\sigma = k^{1/2} l$. The difference from Prandtl's model, which is $\sigma = l^2_m \left| \frac{\partial u}{\partial y} \right|$, is that here both the turbulence energy and length scale are determined by way of transport equations. The difference from the one-equation model is that here the length scale is determined by means of transport equations.

Table 1 is a list of some proposals for the

dependent variable of the length-scale-determining equation. In this work, k-σ model latestly proposed by Stuhmiller is adopted. But his work excludes the effect of gravitational force field on the turbulence. The purpose of this work is to develop a mathematical and numerical model for the turbulent stresses applicable in buoyant-affected turbulence, to show some results of the model and to indicate directions for further extension and refinements.

Table 1. Some Proposals for the Dependent Variable of the Second Equation

Proposer(s), Year	Dependent Variable	Symbol
Kolmogorov (1942)	$k^{1/2}/l$	f
Chou (1945), Davidov (1961) Harlow-Nakayama (1968) Jones-Launder (1972)	$k^{2/3}/l$	ε
Rotta (1951) Spalding (1967)	l	l
Rotta (1968, 1971) Rodi-Spalding (1970) Ng-Spalding (1972)	kl	kl
Spalding (1969)	k/l^2	W
Stuhmiller (1974)	$k^{1/2}\,l$	σ

II. Model Development

This study deals with the two-dimensional time dependent buoyant turbulent fluid mechanics equations of continuity variables and energy for a Boussinesq fluid. Two closure variables, the turbulence kinetic energy and the turbulence viscosity, are also calculated from their own transport equations to give turbulence viscosity, which results in the two-equation turbulence model. The differential equations solved in this study are as follows.

$$\frac{\partial u}{\partial t}+\frac{1}{r}\frac{\partial}{\partial r}ru^2+\frac{\partial(uw)}{\partial z}=-\frac{\partial P}{\partial r}+\frac{(\rho-\rho_0)}{\rho_0}g_r-R_r(u)$$
$$+\frac{\partial}{\partial r}\left[\left(\frac{\sigma}{r}\right)\frac{\partial(ru)}{\partial r}\right]+\frac{\partial}{\partial z}\left[(\sigma)\frac{\partial u}{\partial z}\right], \quad (1)$$

$$\frac{\partial w}{\partial t}+\frac{1}{r}\frac{\partial}{\partial r}ruw+\frac{\partial w^2}{\partial z}=-\frac{\partial p}{\partial z}+\frac{(\rho-\rho_0)}{\rho_0}g_z-R_z(w)$$
$$+\frac{1}{r}\frac{\partial}{\partial r}\left[(r\sigma)\frac{\partial w}{\partial r}\right]+\frac{\partial}{\partial z}\left[(\sigma)\frac{\partial w}{\partial z}\right], \quad (2)$$

$$\frac{\partial k}{\partial t}+\frac{1}{r}\frac{\partial}{\partial r}(ruk)+\frac{\partial}{\partial z}(wk)=+2\sigma(\mathrm{SI})+\tau\left\{\frac{1}{r}\frac{\partial}{\partial r}\left[(r\sigma)\frac{\partial k}{\partial r}\right]+\frac{\partial}{\partial z}\left[(\sigma)\frac{\partial k}{\partial z}\right]\right\}-4\alpha k^2/\sigma, \quad (3)$$

where $\mathrm{SI}=\left(\frac{\partial u}{\partial r}\right)^2+\left(\frac{\partial w}{\partial z}\right)^2+\frac{1}{2}\left(\frac{\partial u}{\partial z}+\frac{\partial w}{\partial r}\right)^2+\frac{u^2}{r^2}$,

$$\frac{\partial \sigma}{\partial t}+\frac{1}{r}\frac{\partial}{\partial r}(ru\sigma)+\frac{\partial}{\partial z}(w\sigma)=+\frac{\sigma^2}{k}(\mathrm{SI})+\tau(\sigma/k)\left\{\frac{1}{r}\frac{\partial}{\partial r}\left[(r\sigma)\frac{\partial k}{\partial r}\right]+\frac{\partial}{\partial z}\left[(\sigma)\frac{\partial k}{\partial z}\right]\right\}-\tau_1\left(\frac{\sigma^3}{k^2}\right)\left\{\frac{1}{r}\frac{\partial}{\partial r}\left[(rk)\frac{\partial}{\partial r}(k/\sigma)\right]+\frac{\partial}{\partial z}\left[(k)\frac{\partial}{\partial z}(k/\sigma)\right]\right\}-\alpha\left(\frac{k}{\sigma}\right)\sigma \quad (4)$$

$$\frac{\partial I}{\partial t}+\frac{1}{r}\frac{\partial}{\partial r}(ruI)+\frac{\partial}{\partial z}(wI)=+\frac{1}{r}\frac{\partial}{\partial r}\left[(r\gamma_T\sigma)\frac{\partial I}{\partial r}\right]+\frac{\partial}{\partial z}\left[(\gamma_T\sigma)\frac{\partial I}{\partial z}\right], \quad (5)$$

$$\frac{1}{r}\frac{\partial(ru)}{\partial r}+\frac{\partial w}{\partial z}=0. \quad (6)$$

In this work, the turbulence parameters α, τ, and τ_1 are set equal to 0.045, 1.5 and 0.75 respectively following the previous recommendation[2].

Eqs. 1 through 6 repesent the momentum equation in the radial direction, the momentum equation in the axial direction, the turbulence

kinetic energy equation, the turbulence viscosity equation, energy equatition and continuity equation respectively. Eqs. 3 and 4 represent k-σ model developed by Stuhmiller. To make this k-σ model take into account the buoyancy effect, the buoyancy production terms of turbulence kinetic equation and the turbulence viscosity equation are developed here. As a starting point for the model development, the term $\beta g_i \overline{u_i' T'}$ is adopted as the buoyant production term of the turbulence kinetic energy equation, where β and g_i represent the fluid temperature coefficient of volume expansion and the acceleration due to gravity respectively. This term has been widely accepted[3] and has proven valid[4] since Spalding and Launder[5] proposed this one. Based on this term, the buoyant production term for the turbulence viscosity equation is derived as follows. By definition

$$\frac{Dk}{Dt} - D(k) = p - \varepsilon, \tag{7}$$

where $D(k)$=diffusion term of k eq.
p =production term of k eq.
ε =dissipation term of k eq.

Rodi[6] has made the following proposals which seem the most popular available at present. The convective and diffusive transport of Reynold stress are supposed to be connected with the kinetic energy transport rates by the formula

$$\frac{D\overline{U_i'U_j'}}{Dt} = \frac{\overline{U_i'U_j'}}{k}\frac{Dk}{Dt}$$

$$D(\overline{U_i'U_j'}) = \frac{\overline{U_i'U_j'}}{k} D(k) \tag{8}$$

This can be modified as follows on the assumption that turbulence kinematic viscosity is roughly proportional to Reynold stress.

$$\frac{D\sigma}{Dt} = \frac{\sigma}{k}\frac{Dk}{Dt}$$

$$D(\sigma) = \frac{\sigma}{k} D(k) \tag{9}$$

From Eq. 7 and 9 one obtains the result:

$$\frac{D\sigma}{Dt} - D(\sigma) = \frac{\sigma}{k}(P - \varepsilon) \tag{10}$$

Therefore we can assume the buoyancy production term of turbulence viscosity equation to be σ/k times that of turbulence kinetic energy equation, i.e., $(\sigma/k)\beta g_i \overline{U_i'T'}$.

For k equation, buoyancy production terms are remodeled as follows and added to the right hand side of Eq. 3.

$$\beta g_i \overline{u_i'T'} = \beta_i \varepsilon_H \frac{\partial T}{\partial x_i}$$

$$= \beta g_i \gamma_T \sigma \frac{\partial T}{\partial x_i}$$

For the σ equation, the buoyancy production term is remodeled as follows and added to the right hand side of Eq. 4.

$$\frac{\sigma}{k} \beta g_i \overline{u'_i T'} = \frac{\sigma}{k} \beta g_i \gamma_T \frac{\partial T}{\partial x_i}$$

III. Solution Methodology

The simplified Marker-and-Cell (SMAC) method[4] is adopted as the fluid mechanics algorithm of this work. The continuity condition that the divergence of a cell is zero is imposed by adjusting the cell pressre. In other words, the cell pressure is changed to counteract the flow. The other importance of this method is that the primitive variables are solved directly with no transformation to vorticity stream function variables.

The complete solution scheme in this work is shown in Fig. 1.

1. One calculational cycle is composed of four steps:

(1) Compute guesses for the new velocities for the entire mesh from the finite difference forms of Eq. 1 and 2 which involve only the values at previous times.

(2) Match the boundary conditions and adjust the new velocities to satisfy the continuity equation by making appropriate changes in the cell pressures. In the iteration, each cell is considered successively and is given a pressure change that drives its velocity divergence to

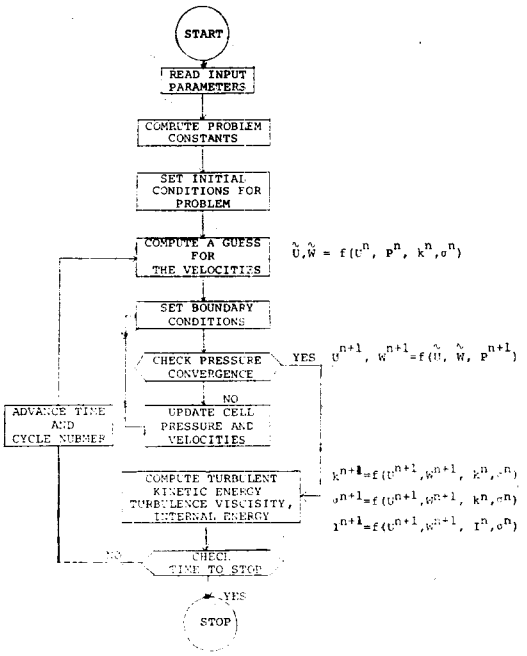

Fig. 1. Flow Diagram of Solution Scheme

zero.

(3) When convergence has been achieved, the velocity and pressure fields are used to compute the turbulence kinetic energy, kinematic viscosity, and internal energy.

(4) Finally, all of the field properties are at the advanced time level and are used as the starting values for the next cycle.

IV. Results

Numerical Experiment

The reactor outlet plenum temperature transient calculation was performed in a cylindrical mesh with ten cells in the radial direction and fifteen cells repressenting the height. Figure 2 shows the test geometry. An obstacle, located in the lower left corner adjacent to the center line, models the inlet pipes through which was input at a flow rate of 1,800 lbm/sec. Flow rate remained constant for all time. The temperature of inlet flow remained at 900°F constant for 100 seconds, but the temperature of the inlet flow dropped from 900°F to 700°F over the next 100 seconds. One outflow cell represented the plenum exit.

Table 2 shows the results that summarize the velocities, turbulence kinetic energy, turbulence kinematic viscosity and temperature of some

Table 2. Results of Negatively-Buoyant LMFBR Outlet Plenum Results

Model Position (I,K)		U (ft/sec)	W (ft/sec)	K (ft/sec)^2	σ (ft^2/sec)	T(°F)
(5, 3)	A	.065	.083	.0747	.115	828
	B	−.069	.794	.0007	.0003	802
(5, 6)	A	.424	.240	.060	.049	836
	B	−.449	.043	10^{-5}	4×10^{-6}	841
(5, 13)	A	.076	.030	.009	.057	895
	B	.140	.167	5×10^{-5}	1.5×10^{-4}	897
(9, 3)	A	.276	.006	.060	.096	820
	B	.143	−.019	10^{-5}	4×10^{-6}	814
(9, 6)	A	−.103	.103	.043	.093	838
	B	−.112	.043	2×10^{-5}	7×10^{-6}	853
(9, 13)	A	.010	−.026	.006	.049	897
	B	−.027	−.109	3×10^{-5}	10^{-4}	896
(10, 3)	A	0.278	0	.055	0.92	832
	B	0.278	0	10^{-5}	3.5×10^{-6}	804

A = k-σ model without buoyant turbulence correction
B = k-σ model with buoyant turbulence correction

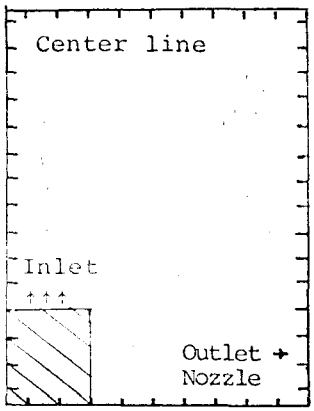

Fig. 2. Configuration of the Reactor Outlet Plenum of Test Problem.

important nodes (including outlet nozzle node which is most concerned) at 100 seconds into the transient.

The results represent two important facts.

First, *the buoyant turbulent correction accounts for a significant increase in the stability of the stratification*. In other words, the temperature difference between the upper hot fluid layers and the cold fluid layers increases.

At the end of the inlet cool-down period (at 100 seconds into the transient) the oustlet nozzle fluid temperature is decreased by the corrections from an uncorrected value of 832°F to a corrected value of 804°F. This is a change of 14% of the original fluid temperature decrease at the plenum inlet. Second, *the turbulence is strongly suppressed*, especially in the inlet zone and thermal interface regions between the stratified hot and cold fluid layers. In other words, there are decreases in both k and σ. This fact leads to the increase in the stability of the stratification.

Comparison with experimental results

A comparison between the predictions and experimental findings is performed. Comparisons are performed based on the temperature variable. At this time, no information is available for velocities and turbulence quantities under non-

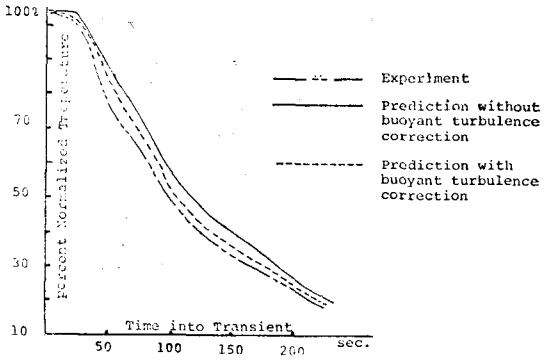

Fig. 3. Experimental and Predieted Temperature of Outlet Nozzle in Test BT 16

isothermal transient conditions for the cases studied. However, the comparison limited to temperature results is fully meaningful because temperature calculation is based on the calculation of the velocity fields and turbulence fields. The comparisons are performed on the basis of using scale-model test data[7] obtained at Argonne National Laboratory (ANL).

Fig. 3 shows the transient temperature prediction at the outlet nozzle for test BT 16 of ANL data. As shown in Fig. 3, the prediction with the buoyancy term on the turbulence transport equation is better than that without the buoyancy term. This fact implies the experimental verification of the improvement of the developed physical and numerical model.

V. Conclusion

It is found that buoyancy strongly affects turbulence in the LMFBR outlet plenum. What is more important, negative buoyancy promotes laminarization during the passage of time in a transient. It is seen that the buoyant suppression of turbulence has the effect of enlarging the lower recirculation zone, of decreasing transverse momentum transport in the inlet region, and reducing mixing of warm fluid in the upper plenum region with incoming cold

fluid. As a result, the predicted thermal shock at the outlet nozzle would be increased significantly by considering the buoyancy effects on turbulent mixing.

References

1. Note on "Turbulent Recirculating Flow-prediction and Measurement," College of Engineering, The Pennsylvania State Univ., July 28-August 1, 1975.
2. J. Stuhmiller, "Development and Validation of a Two Variable Turbulence Model," SAI-74-509-LJ, 1974.
3. Chen, C.J. and W. Rodi, "A Mathematical Model for Stratified Turbulent Flow and its Application to Buoyant Jets," 16th IAHR Congress, Sao Paulo (1975).
4. Ralph G. Bennett, "Numerical Modeling of Buoyant Plumes in a Turbulent, Stratified Atmosphere," Ph.D. Thesis, NED, Massachusetts Institute of Technology, 1979.
5. Launder, B.E. and D.B. Spalding, *Lectures in Mathematical Models of Turbulence*, Academic Press, London and New York, 1972.
6. Rodi, W., "The Prediction of Free Turbulent Boundary Layers by Use of a 2-Equation Model of Turbulence," Ph.D. Thesis, Univ. of London, 1972.
7. P.A. Howard and J.A. Carbajo, Experimental Study of Scram Transients in Generalized Liquid-Metal Fast Breeder Reactor Outlet ,Plenums *Nuclear Technology Vol. 44*, July 1979.